

A neural network approach for two-body systems with spin and isospin degrees of freedom

Chuanxin Wang (王传新)^{1,2} Tomoya Naito (内藤智也)^{2,3,*} Jian Li (李剑)^{1,†} and Haozhao Liang (梁豪兆)^{3,2,‡}

¹College of Physics, Jilin University, Changchun 130012, China

²RIKEN Interdisciplinary Theoretical and Mathematical Sciences Program (iTHEMS), Wako 351-0198, Japan

³Department of Physics, Graduate School of Science,
The University of Tokyo, Tokyo 113-0033, Japan

(Dated: March 26, 2024)

We propose an enhanced machine learning method to calculate the ground state of two-body systems. Compared to the original method [Naito, Naito, and Hashimoto, Phys. Rev. Research **5**, 033189 (2023)], the present method enables one to consider the spin and isospin degrees of freedom by employing a non-fully-connected deep neural network and the unsupervised machine learning technique. The validity of this method is verified by calculating the unique bound state of deuteron.

I. INTRODUCTION

Quantum systems, from atomic nuclei to solids, are composed of many particles, and thus finding states of many-body systems is an essential problem. In advanced quantum many-body methods, such as density functional theory [1–3], tensor network [4, 5], and variational Monte Carlo method [6–8], the ground-state energy can be treated in a variational form, turning finding the ground state of the system into a variational problem. Among the methods for solving the variational problem, the unsupervised machine learning (ML) is gaining attention due to its powerful performance for optimization, making it an ideal tool to solve many-body problems in quantum systems.

In unsupervised ML for variational problems, the ML structure can be treated as a trial function. In the case of quantum many-body systems, the energy expectation value $\langle H \rangle$ with respect to the system Hamiltonian H is treated as the loss function and the output of the ML is usually regarded as the wave function.

For the unsupervised ML application for spin systems, the pioneering work solved both static and time-evolution systems by using the restricted Boltzmann machine as a wave function ansatz [9]. In the following works, the updated algorithms to achieve a higher accuracy [10] and the deterministic time evolution [11] were promoted. The Jastrow-Slater wave function ansatz was also applied to the unsupervised ML technique [12]. The excited-state calculation was presented with two different ansätze [13, 14]. Recently, the transfer matrix for a spin-glass model was calculated by using an unsupervised deep neural network [15].

For continuous systems with many bosons or fermions, the (anti)symmetrization is an important but difficult problem to implement a neural network *directly*. Reference [16] used a small neural network to perform

calculation of deuterons in momentum space, where (anti)symmetrization need not be considered. For bosonic systems, Ref. [17] proposed a neural network to calculate the Calogero-Sutherland model and of the Efimov bound states and Ref. [18] proposed to use a pooling layer to consider the symmetrization. In contrast, for fermionic systems, such as electronic structure of atoms and molecules and nuclear structure with an *ab initio* Hamiltonian, the Jastrow-Slater ansatz is often introduced to consider the fermion antisymmetrization and the interparticle correlation [19–23]. The hidden-fermion technique [24], which is an extension of the Jastrow-Slater ansatz, was proposed and applied with an unsupervised ML. This technique was immediately applied to nuclear systems, e.g., ¹⁶O [25]. Another proposed method to calculate electronic structure was to map the fermionic system into a spin system [26]. The recent progress is summarized in Ref. [27].

The direct method to solve the Schrödinger equation in coordinate space using an unsupervised deep neural network (DNN) for bosonic systems and fermionic systems with the equal footing was proposed in Ref. [28]. According to the universal approximation theorem [29, 30], a neural network can span much larger space of the trial wave functions; since larger space of the trial wave functions leads to more accurate estimation of the ground-state energy in the variational principle, a neural network was used as a trial wave function [28]. The method to calculate the excited states, which has rarely been discussed in previous works, was also introduced in Ref. [28]. By utilizing energy expectation as the loss function for minimization, this method successfully calculated the ground state of one-dimensional (1D) one- to three-body systems. Low-lying excited states were calculated by utilizing the orthonormal condition and the variational principle. However, the spin and isospin degrees of freedom, which are crucial for discussing the properties of magnetic materials and atomic nuclei, were not considered yet.

In this paper, we extend the method proposed in Ref. [28] to include the spin and isospin degrees of freedom. We will mainly focus on the two-body systems

* tnaito@ribf.riken.jp

† jianli@jlu.edu.cn

‡ haozhao.liang@phys.s.u-tokyo.ac.jp

without the external potential. Due to translational symmetry, we only consider the relative motion, which reduces computational complexity.

In detail, we validate our method by calculating the unique two-nucleon bound system—deuteron. A deuteron is the simplest realistic many-body system, where the spin and isospin degrees of freedom play important roles. Since a deuteron has only one bound state, we do not focus on the excited states in the present discussions. In the process of optimization, Ref. [16] used a supervised method to prepare the DNN parameters with artificially selected target wave functions, which is not needed in our method. Reference [16] also pointed out that the extension to arbitrary spin and isospin was a future perspective; our method can be applied to arbitrary spin and isospin by using a non-fully connected DNN structure.

This paper is organized as follows: In Sec. II, we discuss the theory to include the spin and isospin degrees of freedom, and also the center of mass to the previous method with partial wave expansions. The corresponding DNN model is proposed in Sec. III. In Sec. IV, we discuss calculation results of deuteron. Finally, we give the summary and future perspectives in Sec. V.

II. METHOD

A. Hamiltonian for two-body systems with spin and isospin degrees of freedom

In the present study, we consider a general self-bound two-body system with the Hamiltonian expressed in coordinate space as

$$H = -\frac{\hbar^2}{2m_1}\nabla_1^2 - \frac{\hbar^2}{2m_2}\nabla_2^2 + V^{\text{int}}(\mathbf{r}_1, \mathbf{r}_2), \quad (1)$$

where the ∇^2 denotes the Laplacian and the V^{int} denotes the two-body interaction. Since we consider a self-bound system, which has a translational symmetry, the center-of-mass motion can be isolated; hence, we can consider the relative motion only. Then, the problem is truncated into the one-body system. By defining the center of mass M and the reduced mass μ as

$$M = m_1 + m_2, \quad \mu = \frac{m_1 m_2}{m_1 + m_2}, \quad (2)$$

with the center-of-mass and relative coordinates

$$\mathbf{R} = \frac{m_1 \mathbf{r}_1 + m_2 \mathbf{r}_2}{m_1 + m_2}, \quad \mathbf{r} = \mathbf{r}_1 - \mathbf{r}_2, \quad (3)$$

respectively, the Hamiltonian can be split into the center-of-mass part H_R and relative motion part H_r

$$H = H_R + H_r, \quad (4a)$$

$$H_R = -\frac{\hbar^2}{2M}\nabla_R^2, \quad (4b)$$

$$H_r = -\frac{\hbar^2}{2\mu}\nabla_r^2 + V^{\text{int}}(\mathbf{r}). \quad (4c)$$

The center-of-mass part H_R can be omitted since it describes the behavior of a free particle. Thus, we only consider the relative motion part H_r .

For example, we assume that the interaction between particles depends only on the relative distance and that the interaction is spherically symmetric. The wave function can, thus, be expanded using spherical harmonics. The relative motion Hamiltonian of the radial wave function reads

$$H_r = -\frac{\hbar^2}{2\mu}\left(\frac{\partial^2}{\partial r^2} + 2\frac{\partial}{\partial r}\right) + \frac{\hbar^2 l(l+1)}{2\mu r^2} + V^{\text{int}}(r), \quad (5)$$

with l the azimuthal quantum number.

B. Argonne series nucleon-nucleon potentials

Compared to the interaction between two electrons, nuclear interactions are much more complex, including the isospin dependence and the non-central tensor force. In the following, we consider a Hamiltonian with the Argonne V18 (AV18) potential [31] to illustrate the present method. The AV18 potential is a nucleon-nucleon potential with explicit charge dependence and charge asymmetry, and it is composed of 18 operators

$$V^{\text{int}}(r) = \sum_{p=1}^{18} V_p(r) O^p. \quad (6)$$

The term O^p denotes a series of 18 operators. The first 14 operators are charge independent,

$$\begin{aligned} O^{p=1-14} &= \left[1, (\boldsymbol{\sigma}_1 \cdot \boldsymbol{\sigma}_2), S_{12}, (\mathbf{L} \cdot \mathbf{S}), L^2, L^2(\boldsymbol{\sigma}_1 \cdot \boldsymbol{\sigma}_2), (\mathbf{L} \cdot \mathbf{S})^2\right] \\ &\otimes [1, (\boldsymbol{\tau}_1 \cdot \boldsymbol{\tau}_2)], \end{aligned} \quad (7)$$

and the last four break the charge independence,

$$O^{p=15-18} = [1, (\boldsymbol{\sigma}_1 \cdot \boldsymbol{\sigma}_2), S_{12}] \otimes T_{12}, (\tau_{z1} + \tau_{z2}). \quad (8)$$

The operators include the Pauli matrices of spin $\boldsymbol{\sigma}$ and isospin $\boldsymbol{\tau}$, the z -projection of isospin τ_z , the product of orbital angular momentum \mathbf{L} and spin \mathbf{S} , and the tensor operator S_{12} and the isotensor operator T_{12} defined by

$$S_{12} = 3\frac{(\boldsymbol{\sigma}_1 \cdot \mathbf{r})(\boldsymbol{\sigma}_2 \cdot \mathbf{r})}{r^2} - \boldsymbol{\sigma}_1 \cdot \boldsymbol{\sigma}_2, \quad (9a)$$

$$T_{12} = 3\tau_{z1}\tau_{z2} - \boldsymbol{\tau}_1 \cdot \boldsymbol{\tau}_2, \quad (9b)$$

respectively. The $V_p(r)$ are obtained by fitting into the two-nucleon scattering data and the deuteron binding energy [31].

Besides the AV18 potential, for the calculation of the deuteron we will also use the Argonne V8' (AV8') [32] and the Argonne V4' (AV4') [33] potentials. The AV8' potential is a simplified version of the AV18 potential with the number of operators reducing from 18 to 8,

$$O^{p=1-8} = [1, (\boldsymbol{\sigma}_1 \cdot \boldsymbol{\sigma}_2), S_{12}, (\mathbf{L} \cdot \mathbf{S})] \otimes [1, (\boldsymbol{\tau}_1 \cdot \boldsymbol{\tau}_2)]. \quad (10)$$

The AV4' potential is a further simplified version with the number of operators reducing from 8 to 4,

$$O^p = 1-4 = [1, (\boldsymbol{\sigma}_1 \cdot \boldsymbol{\sigma}_2)] \otimes [1, (\boldsymbol{\tau}_1 \cdot \boldsymbol{\tau}_2)]. \quad (11)$$

The radial potentials $V_p(r)$ for both AV8' and AV4' potentials are a linear combination of $V_p(r)$ of the AV18 one.

C. Partial wave expansion of wave function

To find the ground state of the selected Hamiltonian, we rewrite the quantum state using the partial wave expansion

$$\begin{aligned} |\Psi\rangle &= \sum_{\substack{L,m_L,S, \\ m_S,T,m_T}} a_{Lm_LSm_S Tm_T} \varphi_{Lm_LSm_S Tm_T} Y_{Lm_L} |Sm_S\rangle \otimes |Tm_T\rangle. \end{aligned} \quad (12)$$

The $\varphi_{Lm_LSm_S Tm_T}$ denotes the radial part of the wave function. The Y_{Lm_L} , $|Sm_S\rangle$, and $|Tm_T\rangle$ are the eigenstates of operators \mathbf{L}^2 , \mathbf{S}^2 , and \mathbf{T}^2 , respectively. We assume partial wave functions are normalized, i.e.,

$$\sum_{\substack{L,m_L,S, \\ m_S,T,m_T}} a_{Lm_LSm_S Tm_T}^2 = 1. \quad (13)$$

Because there exists the $(\mathbf{L} \cdot \mathbf{S})$ term in the AV18 and AV8' potentials, the quantum numbers $L(L+1)$ and $S(S+1)$ are no longer good quantum numbers. Therefore, we introduce the new good quantum number $J(J+1)$, which is the eigenvalue of the operator $\mathbf{J} = \mathbf{L} + \mathbf{S}$. By changing the basis of partial waves, the new expansion of the wave function reads

$$\begin{aligned} |\Psi\rangle &= \sum_{\substack{L,m_L,S, \\ m_S,T,m_T}} a_{Lm_LSm_S Tm_T} \varphi_{Lm_LSm_S Tm_T} Y_{Lm_L} |Sm_S\rangle \otimes |Tm_T\rangle \\ &= \sum_{\substack{L,S,J, \\ m_J,T,m_T}} b_{LSJm_J Tm_T} \psi_{LSJm_J Tm_T} |LSJm_J\rangle \otimes |Tm_T\rangle \end{aligned} \quad (14)$$

with the normalization condition for the new coefficients

$$\sum_{\substack{L,S,J, \\ m_J,T,m_T}} b_{LSJm_J Tm_T}^2 = 1. \quad (15)$$

By utilizing the Clebsch-Gordan coefficients $c_{j_1 m_{j_1} j_2 m_{j_2}}^{J m_J}$, we have the expansion

$$|LSJm_J\rangle = \sum_{m_L, m_S} c_{Lm_L Sm_S}^{Jm_J} Y_{Lm_L} |Sm_S\rangle. \quad (16)$$

Because the deuteron is an isospin singlet state, we only consider $|Tm_T\rangle = |00\rangle$ and omit it in the following. Therefore, the wave function can be simplified as

$$|\Psi\rangle = \sum_{\substack{L,S, \\ J,m_J}} b_{LSJm_J 00} \psi_{LSJm_J 00} \sum_{m_L, m_S} c_{Lm_L Sm_S}^{Jm_J} Y_{Lm_L} |Sm_S\rangle. \quad (17)$$

Because of the $SO(3)$ symmetry for J , the states with different m_J degenerate

$$d_{LSJ} \phi_{LSJ} = \sum_{m_J} b_{LSJm_J 00} \psi_{LSJm_J 00}. \quad (18)$$

The final partial wave expansion is

$$|\Psi\rangle = \sum_{L,S,J} d_{LSJ} \phi_{LSJ} \sum_{m_L, m_S, m_J} c_{Lm_L Sm_S}^{Jm_J} Y_{L, m_L} |Sm_S\rangle \quad (19)$$

with the normalization condition

$$\sum_{L,S,J} d_{LSJ}^2 (2J+1) = 1. \quad (20)$$

III. NEURAL NETWORK MODELS

A. The discrete forms of Hamiltonian and wave functions in neural network

In the present neural network approach, the wave function is represented by a DNN. Because we focus on the bound states of systems only, it is enough to calculate the system within a box of finite size. We discretize the spatial coordinate r as the input variables and the partial wave functions $\phi_{LSJ}(r)$ as the output variables of DNN so that they can be represented as vectors. The mesh points of spatial coordinates are evenly distributed with size Δr , with M mesh points in total. Because the centrifugal potential diverges at the origin and the Dirichlet boundary condition is introduced, the actual number of mesh points used for the calculation is $M-1$. The vector corresponding to the radial partial wave function ϕ_{LSJ} of Eq. (19) reads

$$\phi_{LSJ} \simeq \begin{pmatrix} \tilde{\phi}_{LSJ1} \\ \tilde{\phi}_{LSJ2} \\ \tilde{\phi}_{LSJ3} \\ \vdots \\ \tilde{\phi}_{LSJ(M-3)} \\ \tilde{\phi}_{LSJ(M-2)} \\ \tilde{\phi}_{LSJ(M-1)} \end{pmatrix}, \quad (21)$$

where the i -th component is

$$\tilde{\phi}_{LSJi} = \phi_{LSJ}(r_i), \quad (22)$$

with $r_i = i \Delta r$.

In the Hamiltonian of Eq. (5), there are the second and first orders of derivatives. These operators are expressed as matrices, which have the following forms

$$\frac{\partial^2}{\partial r^2} \simeq \frac{1}{(\Delta r)^2} \begin{pmatrix} -2 & 1 & 0 & \dots & 0 & 0 & 0 \\ 1 & -2 & 1 & \dots & 0 & 0 & 0 \\ 0 & 1 & -2 & \dots & 0 & 0 & 0 \\ \vdots & \vdots & \vdots & \ddots & \vdots & \vdots & \vdots \\ 0 & 0 & 0 & \dots & -2 & 1 & 0 \\ 0 & 0 & 0 & \dots & 1 & -2 & 1 \\ 0 & 0 & 0 & \dots & 0 & 1 & -2 \end{pmatrix} \quad (23)$$

and

$$\frac{\partial}{\partial r} \simeq \frac{1}{2\Delta r} \begin{pmatrix} 0 & 1 & 0 & \dots & 0 & 0 & 0 \\ -1 & 0 & 1 & \dots & 0 & 0 & 0 \\ 0 & -1 & 0 & \dots & 0 & 0 & 0 \\ \vdots & \vdots & \vdots & \ddots & \vdots & \vdots & \vdots \\ 0 & 0 & 0 & \dots & 0 & 1 & 0 \\ 0 & 0 & 0 & \dots & -1 & 0 & 1 \\ 0 & 0 & 0 & \dots & 0 & -1 & 0 \end{pmatrix}, \quad (24)$$

respectively. The radial part of the interaction V_p and centrifugal potential, denoted as V altogether, are expressed as diagonal matrices

$$V \simeq \begin{pmatrix} \tilde{V}_1 & 0 & 0 & \dots & 0 & 0 & 0 \\ 0 & \tilde{V}_2 & 0 & \dots & 0 & 0 & 0 \\ 0 & 0 & \tilde{V}_3 & \dots & 0 & 0 & 0 \\ \vdots & \vdots & \vdots & \ddots & \vdots & \vdots & \vdots \\ 0 & 0 & 0 & \dots & \tilde{V}_{M-3} & 0 & 0 \\ 0 & 0 & 0 & \dots & 0 & \tilde{V}_{M-2} & 0 \\ 0 & 0 & 0 & \dots & 0 & 0 & \tilde{V}_{M-1} \end{pmatrix}, \quad (25)$$

where $\tilde{V}_i = V(r_i)$. The ground-state energy E_0 can then be calculated by

$$E_0 \simeq \frac{\langle \Psi | H | \Psi \rangle}{\langle \Psi | \Psi \rangle}. \quad (26)$$

B. The design of the non-fully-connected neural network

The design of the present non-fully-connected DNN, which generates partial waves of the wave functions, is shown in Fig. 1. The input is the relative distance r_i . The outputs are the partial wave functions. After determining the cutoff value of the orbital angular momentum L and the spin quantum number S , the possible angular momentum sets $\{LSJ\}$ of partial waves are then decided by the LS coupling. For each single output, the nodes in the hidden layers are fully connected, while the hidden layer nodes of different outputs are not connected to each other. The ‘‘softplus’’ function

$$\text{softplus}(x) = \log(1 + e^x) \quad (27)$$

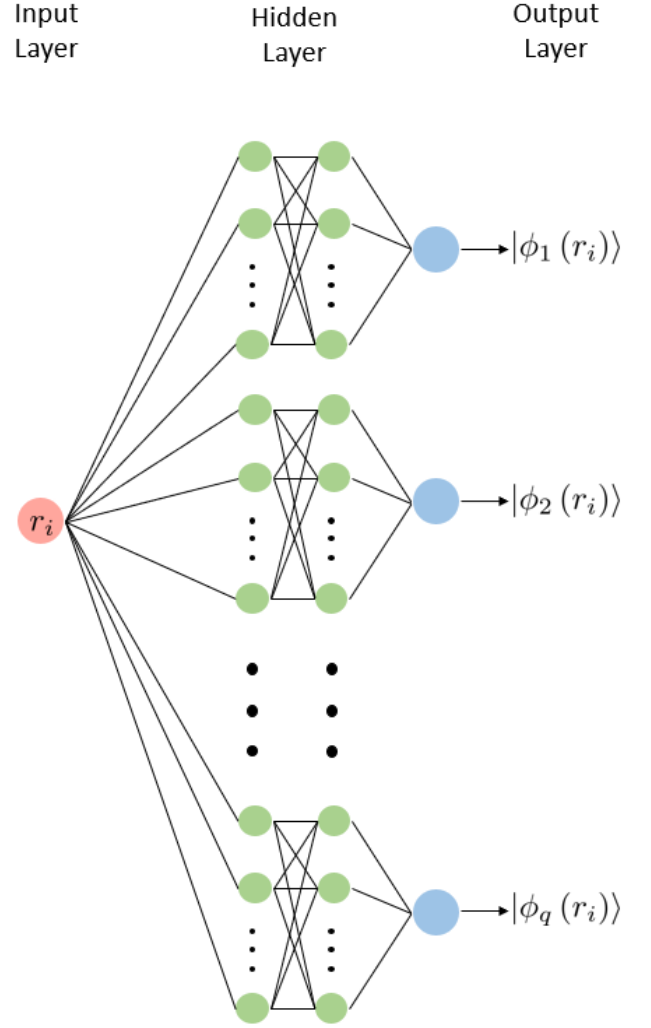


FIG. 1. Schematic figure of the non-fully-connected deep neural network. The shared input is the relative distance between the particles. The output are the partial wave functions ϕ_j , where j ($j = 1, 2, \dots, q$) represents the combination of the angular momenta, L , S , and J . There is no connection between hidden layer nodes of different outputs. The computational accuracy can be enhanced by increasing the number of layers and nodes in each layer.

is used as the activation function.

Throughout the training process, the relative distances of the particles are discretized into M uniformly distributed lattice points, which are passed to the DNN as a dataset. The output of the DNN is a dataset containing all the partial wave functions. The energy expectation value is regarded as the loss function, which is calculated from Eq. (26). The parameters of DNN are then updated by the Adam optimizer [34] and the ML is implemented by using the TENSORFLOW [35].

IV. CALCULATION RESULTS FOR DEUTERON

We validate the feasibility of the method by applying it to deuteron. To include a more general case, at the beginning, we consider the orbital angular momentum L from zero to four and spin S from zero to one in Eq. (22), with 18 possible states in total. The 18 partial wave functions are computed in a 20 fm box with 4000 mesh points. The DNN used is composed of two layers each containing 16 units. We train the model to testify whether only the 3S_1 and 3D_1 states are obtained, which is a known fact for the properties of deuteron [36]. The contributions of each state to the total energy are listed in Table I. The results show that only the 3S_1 and 3D_1 states make significant contributions in the ground state, while the contributions of the other states is small enough to be neglected, which is consistent with the known fact. The relative error of the ground-state energy is 0.05% of the benchmark value shown in Ref. [31].

Since we have proven that only the 3S_1 and 3D_1 states contribute to the ground-state energy, we can reduce the number of outputs from 18 to two to reduce the size of the DNN. Accordingly, the calculation cost is also reduced; hence, hereinafter we use a 30 fm box with 6000 mesh points, and a more complicated hidden layer structure that is composed of three layers each containing 16 units. The energies obtained with the AV18, AV8', and AV4' potentials are listed in Table II. The accuracy is both within 5 keV (0.05%) for AV18 and AV8' calculations compared to the benchmark [31]. AV4' potential includes only four terms without the electromagnetic (EM) interaction between a proton and a neutron; accordingly the final error reaches about 1% error [33]. Figure 2 shows the deuteron wave functions based on AV18 and AV8' potentials, which are compared with deuteron wave functions of the AV18 calculation in Ref. [31]. We observe that the DNN results of both AV18 and AV8' calculations reproduce the AV18 benchmark [31] quite nicely. The only region where small differences are visible is near the origin ($r \lesssim 0.05$ fm). The relative error $[u^{\text{DNN}}(r) - u^{\text{benchmark}}(r)]/u^{\text{benchmark}}(r)$ and $[w^{\text{DNN}}(r) - w^{\text{benchmark}}(r)]/w^{\text{benchmark}}(r)$ are shown in Fig. 3, where u and w are the wave functions of 3S_1 and 3D_1 states, respectively. The main origin of the error is due to the 3D_1 state because it converges to zero at $r = 0$ and the large r .

Table III shows the performance of the program by varying the number of layers and nodes with the AV8' potential. In the case of a single hidden layer containing eight units, the relative error of energy reaches 2%. With increasing the number of units to 16 or adding a hidden layer, the relative errors do not exceed 0.03%. A more complicated network structure does not bring higher precision, since the training results fluctuate slightly every time.

Figure 4 shows the relative error of the loss function to the benchmark energy as a function of epochs in the

TABLE I. Contributions of 18 partial wave states to the deuteron ground-state energy with the AV8' potential. The ground-state energy reads -2.2232 MeV which is within 0.05% relative error to the benchmark value [31]. Each unconnected hidden layers are two layers, each of which is composed of 16 units.

		$S = 1$	$S = 0$
$L = 0$	$J = 0$		4.9028×10^{-8}
	$J = 1$	0.9423	
$L = 1$	$J = 0$	1.2063×10^{-8}	
	$J = 1$	9.3094×10^{-9}	8.0052×10^{-9}
	$J = 2$	1.8498×10^{-9}	
$L = 2$	$J = 1$	0.0577	
	$J = 2$	2.8180×10^{-10}	2.7747×10^{-8}
	$J = 3$	2.9663×10^{-9}	
$L = 3$	$J = 2$	3.1013×10^{-8}	
	$J = 3$	2.6941×10^{-9}	3.0312×10^{-9}
	$J = 4$	5.3381×10^{-9}	
$L = 4$	$J = 3$	7.9230×10^{-10}	
	$J = 4$	4.1554×10^{-9}	2.0494×10^{-8}
	$J = 5$	2.7268×10^{-8}	

TABLE II. DNN results for the energies of the deuteron in the AV18, AV8' (with and without electromagnetic terms), and AV4' potentials. There exist about 1% relative errors in the AV8' (without EM terms) and AV4' results. The hidden layers of each output are composed of three layers each of which has 16 units. The benchmark energy is taken from Ref. [31].

	Energy (MeV)	Relative Error
Benchmark (AV18) [31]	-2.2245	
AV18 (with EM)	-2.2252	0.032%
AV8' (with EM)	-2.2247	0.008%
AV8' (without EM)	-2.2413	0.755%
AV4' (without EM)	-2.2435	0.854%

AV8' calculation. The fluctuation appears at about 5000 iterations. Although the highest precision reaches 1.0×10^{-7} , the final result is about 1.0×10^{-4} . The reason is the *exact* result with discretization is slightly lower than the benchmark deuteron energy due to the discretization.

V. SUMMARY

In Ref. [28], an unsupervised machine learning technique is developed to calculate the ground and low-lying excited states with deep neural network. In this paper, we extend the method by introducing the spin and isospin degrees of freedom through the introduction of partial wave expansions, which are generated by a non-fully-connected deep neural network.

We verified the method by calculating the simplest two-body nuclear system—deuteron. At first, the partial waves with the orbital angular momentum L from

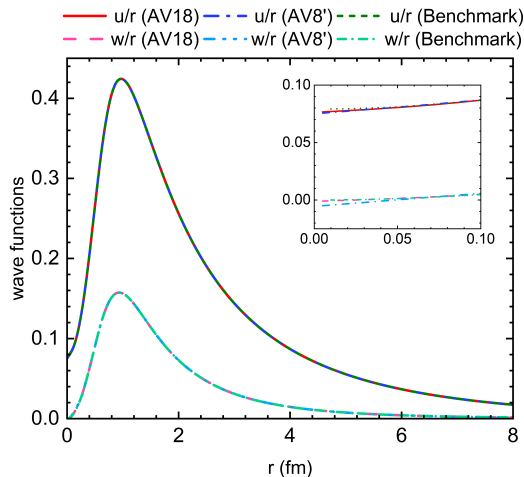


FIG. 2. Deuteron wave functions with the AV18 and AV8' potentials, where u/r and w/r denote the wave functions of the 3S_1 and 3D_1 states, respectively. The benchmark are based on the AV18 calculation [31]. The hidden layers of each output are composed of three layers each of which has 16 units. Almost all lines overlap with each other except for the slight differences near the origin within 0.05 fm as shown in the insert.

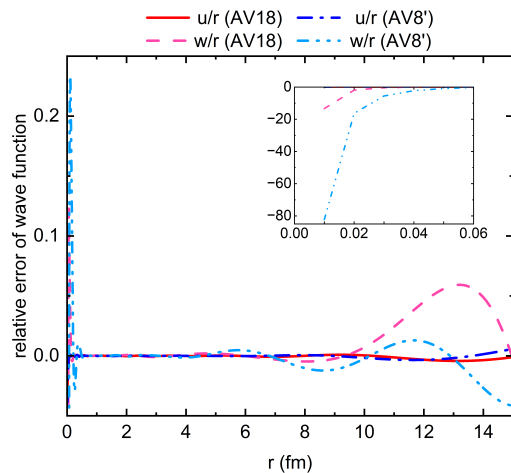


FIG. 3. Relative error of DNN deuteron wave functions to the AV18 benchmark results [31]. The hidden layers of each output are composed of three layers each of which has 16 units.

zero to four and the possible total spin S from zero to one are calculated. The results are consistent with the known fact, i.e., only the 3S_1 and 3D_1 states contribute to the deuteron ground state. In the following calculations, the obtained wave functions and energies show consistency with the corresponding results of benchmark [31, 33]. We find that the deep neural network does not need to be large. In the present case, two hidden layers and each of them containing eight units are sufficient to

TABLE III. Performance test of the deuteron calculation in the AV8' potential. Row with “—” in the column “# of unit in layers” represents an empty layer. The benchmark exact values are listed in the last row.

# of Unit in Layers			Energy	Relative Error	D state prob.
1st	2nd	3rd	(MeV)		
8	—	—	-2.17846	2.071 %	5.71 %
16	—	—	-2.22525	0.026 %	5.76 %
8	8	—	-2.22495	0.017 %	5.76 %
8	16	—	-2.22475	0.007 %	5.76 %
16	8	—	-2.22512	0.027 %	5.76 %
16	16	—	-2.22454	0.002 %	5.76 %
8	8	8	-2.22498	0.018 %	5.76 %
16	16	16	-2.22477	0.008 %	5.76 %
Exact [31]			-2.22458		5.76 %

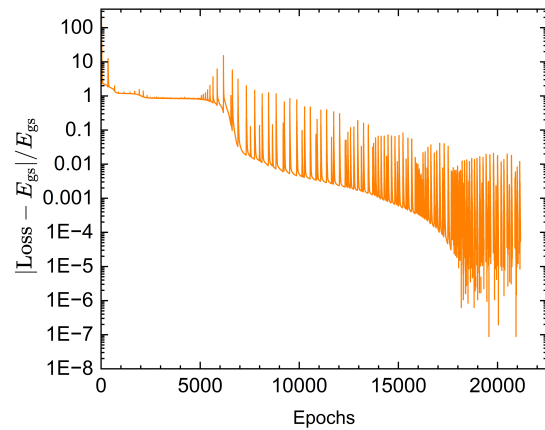


FIG. 4. Relative error of $\langle H \rangle$ with respect to the exact ground-state energy E_{gs} with the AV8' potential as the functions of the number of epochs. The hidden layers of each output are composed of three layers each of which has 16 units.

generate faithful representations of the wave function.

We believe that these improvements to the deep neural network approach hold promise for more studies that could further extend the methodology of this work. For example, one is to extend from two-body calculations to N -body calculations. In particular, Jacobi coordinates are a geometrical description of a N -body system with $(3N - 6)$ internal coordinates [37], which might turn out to be applicable to our deep neural network method for many-body systems and significantly lower computation resources than in Cartesian coordinates. Another is to perform the calculations within the relativistic scheme. The relativistic effects can be well described by, for example, the CD-Bonn potential, which is fitted to the empirical value for the deuteron binding energy [38].

ACKNOWLEDGMENTS

The authors thank Koji Hashimoto and Hisashi Naito for the fruitful discussion. C.W. acknowledges the warm hospitality of the RIKEN iTHEMS program. T.N. acknowledges the RIKEN Special Postdoctoral Researcher Program, the JSPS Grant-in-Aid for Research Activity Start-up under Grant No. JP22K20372, the JSPS Grant-in-Aid for Transformative Research Areas (A) under Grant No. JP23H04526, the JSPS Grant-in-Aid for Scientific Research (B) under Grant No. JP23H01845, and

the JSPS Grant-in-Aid for Scientific Research (C) under Grant No. JP23K03426. J.L. acknowledges the National Natural Science Foundation of China (No. 11675063) and the Natural Science Foundation of Jilin Province (No. 20220101017JC). H.L. acknowledges the JSPS Grant-in-Aid for Scientific Research (S) under Grant No. JP20H05648 and the RIKEN Pioneering Project: Evolution of Matter in the Universe. The numerical calculations were performed on cluster computers at the RIKEN iTHEMS program.

-
- [1] P. Hohenberg and W. Kohn, Inhomogeneous Electron Gas, *Phys. Rev.* **136**, B864 (1964).
- [2] W. Kohn and L. J. Sham, Self-Consistent Equations Including Exchange and Correlation Effects, *Phys. Rev.* **140**, A1133 (1965).
- [3] W. Kohn, Nobel Lecture: Electronic structure of matter—wave functions and density functionals, *Rev. Mod. Phys.* **71**, 1253 (1999).
- [4] S. R. White, Density matrix formulation for quantum renormalization groups, *Phys. Rev. Lett.* **69**, 2863 (1992).
- [5] H. Shinaoka, D. Geffroy, M. Wallerberger, J. Otsuki, K. Yoshimi, E. Gull, and J. Kuneš, Sparse sampling and tensor network representation of two-particle Green's functions, *SciPost Phys.* **8**, 012 (2020).
- [6] W. L. McMillan, Ground State of Liquid He⁴, *Phys. Rev.* **138**, A442 (1965).
- [7] D. Ceperley, G. V. Chester, and M. H. Kalos, Monte Carlo simulation of a many-fermion study, *Phys. Rev. B* **16**, 3081 (1977).
- [8] D. M. Ceperley and B. J. Alder, Ground State of the Electron Gas by a Stochastic Method, *Phys. Rev. Lett.* **45**, 566 (1980).
- [9] G. Carleo and M. Troyer, Solving the quantum many-body problem with artificial neural networks, *Science* **355**, 602 (2017).
- [10] Y. Nomura, A. S. Darmawan, Y. Yamaji, and M. Imada, Restricted Boltzmann machine learning for solving strongly correlated quantum systems, *Phys. Rev. B* **96**, 205152 (2017).
- [11] G. Carleo, Y. Nomura, and M. Imada, Constructing exact representations of quantum many-body systems with deep neural networks, *Nat. Commun.* **9**, 5322 (2018).
- [12] J. Stokes, J. R. Moreno, E. A. Pnevmatikakis, and G. Carleo, Phases of two-dimensional spinless lattice fermions with first-quantized deep neural-network quantum states, *Phys. Rev. B* **102**, 205122 (2020).
- [13] K. Choo, G. Carleo, N. Regnault, and T. Neupert, Symmetries and Many-Body Excitations with Neural-Network Quantum States, *Phys. Rev. Lett.* **121**, 167204 (2018).
- [14] Y. Nomura, Machine Learning Quantum States — Extensions to Fermion-Boson Coupled Systems and Excited-State Calculations, *J. Phys. Soc. Jpn.* **89**, 054706 (2020).
- [15] H. Yoshino, Spatially heterogeneous learning by a deep student machine, *Phys. Rev. Research* **5**, 033068 (2023).
- [16] J. W. T. Keeble and A. Rios, Machine learning the deuteron, *Phys. Lett. B* **809**, 135743 (2020).
- [17] H. Saito, Method to Solve Quantum Few-Body Problems with Artificial Neural Networks, *J. Phys. Soc. Jpn.* **87**, 074002 (2018).
- [18] G. Pescia, J. Han, A. Lovato, J. Lu, and G. Carleo, Neural-network quantum states for periodic systems in continuous space, *Phys. Rev. Research* **4**, 023138 (2022).
- [19] D. Pfau, J. S. Spencer, A. G. D. G. Matthews, and W. M. C. Foulkes, *Ab initio* solution of the many-electron Schrödinger equation with deep neural networks, *Phys. Rev. Research* **2**, 033429 (2020).
- [20] J. Hermann, Z. Schätzle, and F. Noé, Deep-neural-network solution of the electronic Schrödinger equation, *Nat. Chem.* **12**, 891 (2020).
- [21] C. Adams, G. Carleo, A. Lovato, and N. Rocco, Variational Monte Carlo Calculations of $A \leq 4$ Nuclei with an Artificial Neural-Network Correlator Ansatz, *Phys. Rev. Lett.* **127**, 022502 (2021).
- [22] A. Gnech, C. Adams, N. Brawand, G. Carleo, A. Lovato, and N. Rocco, Nuclei with Up to $A = 6$ Nucleons with Artificial Neural Network Wave Functions, *Few-Body Syst.* **63**, 7 (2022).
- [23] Y. L. Yang and P. W. Zhao, Deep-neural-network approach to solving the *ab initio* nuclear structure problem, *Phys. Rev. C* **107**, 034320 (2023).
- [24] J. R. Moreno, G. Carleo, A. Georges, and J. Stokes, Fermionic wave functions from neural-network constrained hidden states, *Proc. Natl. Acad. Sci. USA* **119**, e2122059119 (2022).
- [25] A. Lovato, C. Adams, G. Carleo, and N. Rocco, Hidden-nucleons neural-network quantum states for the nuclear many-body problem, *Phys. Rev. Research* **4**, 043178 (2022).
- [26] K. Choo, A. Mezzacapo, and G. Carleo, Fermionic neural-network states for *ab-initio* electronic structure, *Nat. Commun.* **11**, 2368 (2020).
- [27] J. Hermann, J. Spencer, K. Choo, A. Mezzacapo, W. M. C. Foulkes, D. Pfau, G. Carleo, and F. Noé, *Ab initio* quantum chemistry with neural-network wavefunctions, *Nat. Rev. Chem.* **7**, 692 (2023).
- [28] T. Naito, H. Naito, and K. Hashimoto, Multi-body wave function of ground and low-lying excited states using unornamented deep neural networks, *Phys. Rev. Research* **5**, 033189 (2023).
- [29] K. Hornik, M. Stinchcombe, and H. White, Multilayer feedforward networks are universal approximators, *Neural Netw.* **2**, 359 (1989).

- [30] K. Hornik, Approximation capabilities of multilayer feed-forward networks, *Neural Netw.* **4**, 251 (1991).
- [31] R. B. Wiringa, V. G. J. Stoks, and R. Schiavilla, Accurate nucleon-nucleon potential with charge-independence breaking, *Phys. Rev. C* **51**, 38 (1995).
- [32] B. S. Pudliner, V. R. Pandharipande, J. Carlson, S. C. Pieper, and R. B. Wiringa, Quantum Monte Carlo calculations of nuclei with $A \leq 7$, *Phys. Rev. C* **56**, 1720 (1997).
- [33] R. B. Wiringa and S. C. Pieper, Evolution of Nuclear Spectra with Nuclear Forces, *Phys. Rev. Lett.* **89**, 182501 (2002).
- [34] D. P. Kingma and J. Ba, Adam: A Method for Stochastic Optimization, in *3rd International Conference on Learning Representations, ICLR 2015, San Diego, CA, USA, May 7-9, 2015, Conference Track Proceedings*, edited by Y. Bengio and Y. LeCun (2015) arXiv:1412.6980 [cs.LG].
- [35] M. Abadi, A. Agarwal, P. Barham, E. Brevdo, Z. Chen, C. Citro, G. S. Corrado, A. Davis, J. Dean, M. Devin, S. Ghemawat, I. Goodfellow, A. Harp, G. Irving, M. Isard, Y. Jia, R. Jozefowicz, L. Kaiser, M. Kudlur, J. Levenberg, D. Mané, R. Monga, S. Moore, D. Murray, C. Olah, M. Schuster, J. Shlens, B. Steiner, I. Sutskever, K. Talwar, P. Tucker, V. Vanhoucke, V. Vasudevan, F. Viégas, O. Vinyals, P. Warden, M. Wattenberg, M. Wicke, Y. Yu, and X. Zheng, TensorFlow: Large-Scale Machine Learning on Heterogeneous Systems (2015), software available from tensorflow.org.
- [36] C. A. Bertulani, *Nuclear Physics in a Nutshell* (Princeton University Press, Princeton, New Jersey, 2007).
- [37] C. Iung, F. Gatti, A. Viel, and X. Chapuisat, Vector parametrization of the N -atom problem in quantum mechanics with non-orthogonal coordinates, *Phys. Chem. Chem. Phys.* **1**, 3377 (1999).
- [38] R. Machleidt, High-precision, charge-dependent Bonn nucleon-nucleon potential, *Phys. Rev. C* **63**, 024001 (2001).